

II. THE PROBLEM

All modern chemical rocket propulsion systems work using the same basic principle—utilizing the law of conservation of momentum to propel a rocket by converting the high temperatures and pressures of a confined combustion reaction into kinetic energy. This conversion is usually carried out in a device called the nozzle, and in most cases, a supersonic converging-diverging (CD) nozzle. Figure 1 shows the relative inefficiency of rocket engines using CD nozzles. A more efficient nozzle, characterized by having a higher specific impulse (I_{sp}), is hoped to be discovered using geometric search techniques, in a manner similar to that generative design (Figure 2).

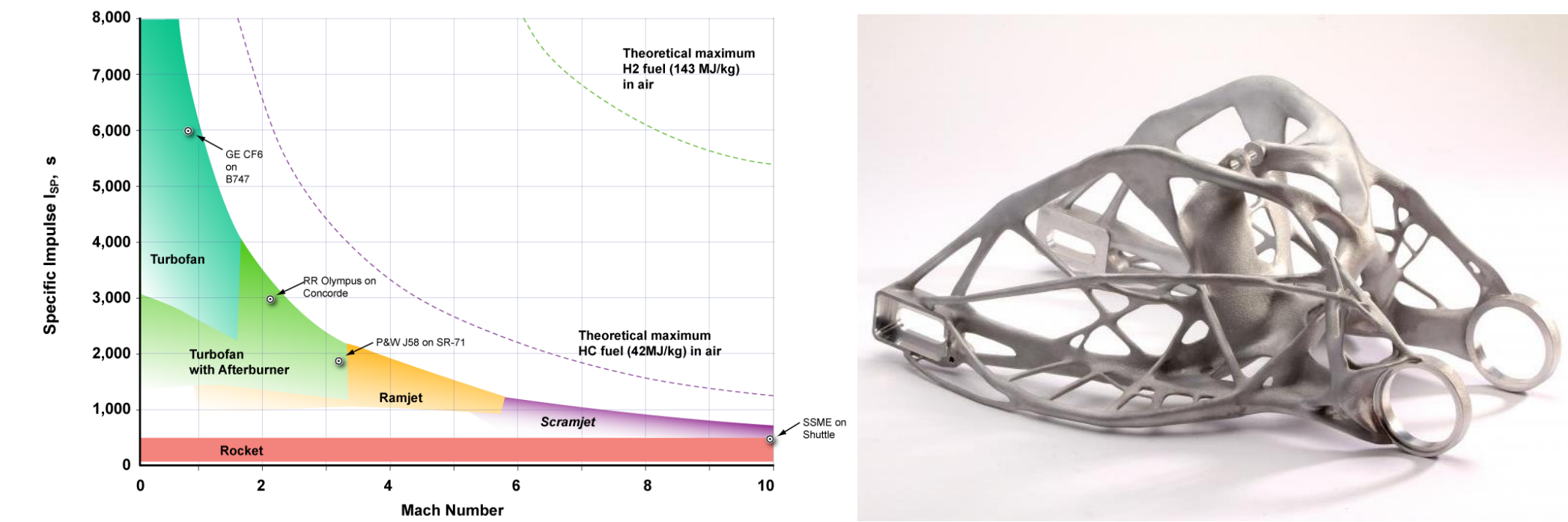


Figure 1: I_{sp} of various common propulsion systems (Wikipedia).

Figure 2: Example of a generatively designed part (Autodesk).

The ramifications of even a slight increase in I_{sp} include millions of dollars saved in launch costs and shorter transit times to Mars.

III. APPROACH & METHODS

Two optimization algorithms were considered: differential evolution (DE) and deep reinforcement learning. DE was chosen since it did not require a convex objective function and was easily applicable for multi-objective purposes. The basic algorithm of DE is as follows (Figure 6):

1) Generate a diverse initial vector population that covers the entire search space. 2) Calculate the fitness (a measure of how optimal of a solution a vector is) value of each member. 3) Select two random vectors and find their difference. 4) Add this new vector to another vector, making a mutated vector. 5) Compare a random trial vector to this vector and perform crossover. 6) Due

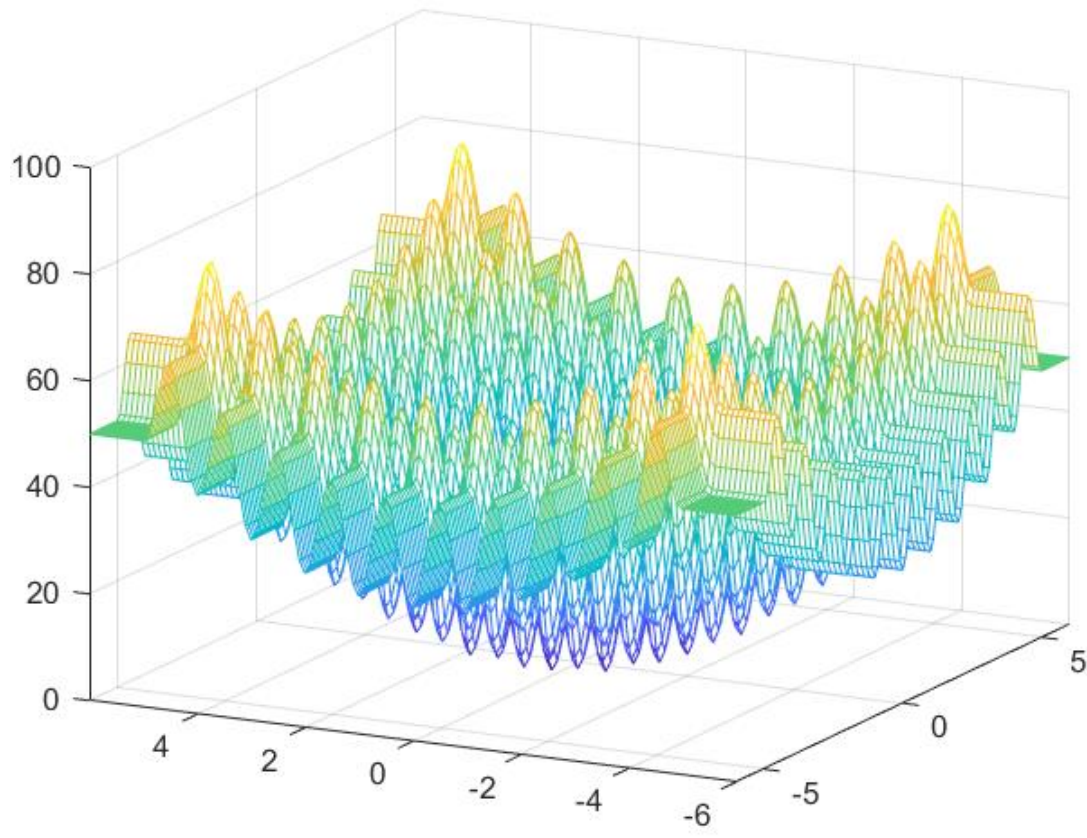


Figure 3: The Rastrigin function.

to the multi-objective nature of DE, this final vector is selected onto the next generation if and only if it is superior in all objective functions. This DE implementation was first tested with the Rastrigin function (2).

$$\nu(M) = \sqrt{\frac{\gamma+1}{\gamma-1}} \tan^{-1} \sqrt{\frac{\gamma-1}{\gamma+1} (M^2 - 1)} - \tan^{-1} \sqrt{M^2 - 1}$$

$$\dot{m} = \frac{P_0 A^*}{\sqrt{T_0}} \sqrt{\frac{\gamma}{R} \left(\frac{2}{\gamma+1} \right)^{\frac{\gamma+1}{\gamma-1}}} \frac{A_t}{A^*} = \frac{1}{M} \left[\frac{2}{\gamma+1} \left(1 + \frac{\gamma-1}{2} M^2 \right) \right]^{\frac{\gamma+1}{2(\gamma-1)}}$$

Figure 4: Critical flow equations: Prandtl-Meyer, choked flow, Mach-area relation.

Next, a fast yet accurate approximation of the ground-truth fitness value (which could be computed using computational fluid dynamics [CFD], i.e. ANSYS Fluent) was needed in order to iterate through the first few hundreds of generations with relative haste, as the initial population is, by nature, noisy. This pseudo-fitness value was computed using both isentropic and shock equations, the most important of which are shown in Figure 3. More specifically, the pseudo-fitness functions

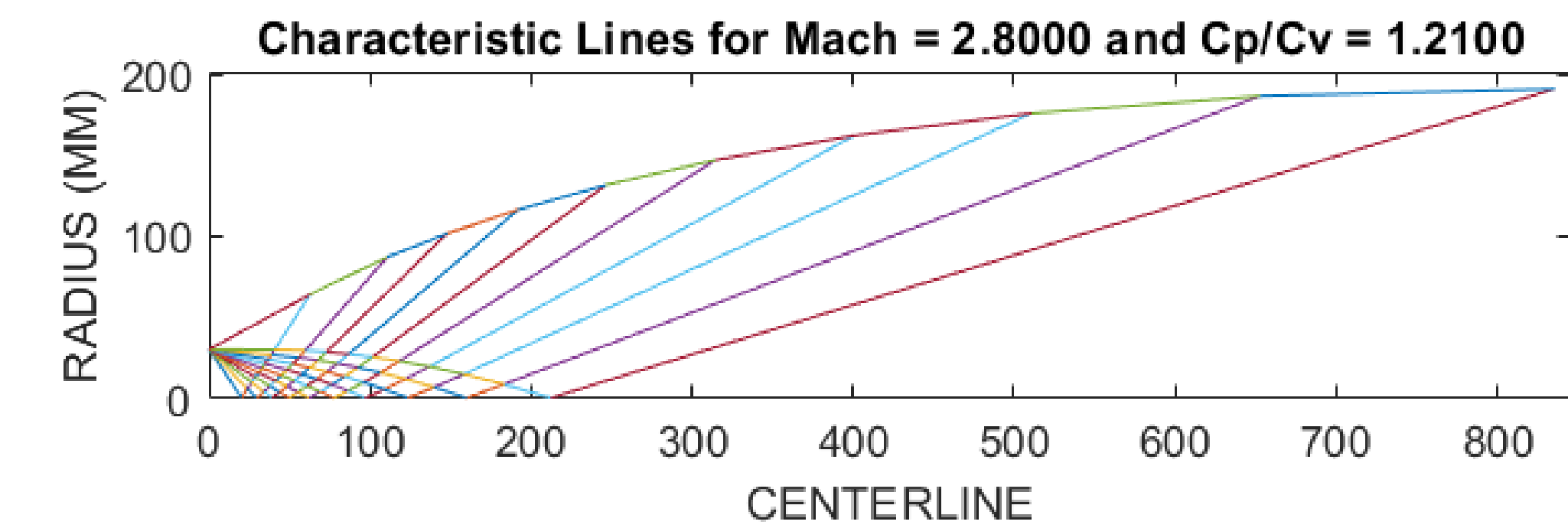


Figure 5: Method of Characteristics, propagates Prandtl-Meyer expansion fans.

Design of a Novel Supersonic Nozzle Using a Multi-Objective Differential Evolution Framework

I. PROJECT OVERVIEW

The aerospace and launch vehicle industry has seen an exciting resurgence in growth and commercialization in recent years. A focal point of design has always been on rocket propulsion systems to both lower costs and increase payload capabilities, whether that be through innovative propellant combinations or new plumbing cycles. However, one critical factor of all rocket engines—the over 130-year-old de Laval nozzle—has hardly changed since its inception. This project aims to reinvent the rocket nozzle using modern search techniques to explore the near infinite geometric search space for a new, optimal geometry. Differential Evolution (DE) was the chosen optimization technique since it not require a differentiable cost function and is easily implementable for multi-objective purposes. My approach was to generate an initially large and diverse population of nozzle geometries and iterate through a specified number of generations using a rudimentary cost function. This cost function is multi-objective and accounts for factors such as the final exhaust velocity, the sum of squared pressure gradients, and the number of strong shocks. It is calculated through isentropic flow relations when the flow is subsonic, and shock/expansion fan propagation once the flow becomes supersonic. After a certain threshold is reached, the remaining generations of geometries are evolved with an automated version of the popular CFD program, ANSYS Fluent, as the cost function.

I. Initial Population

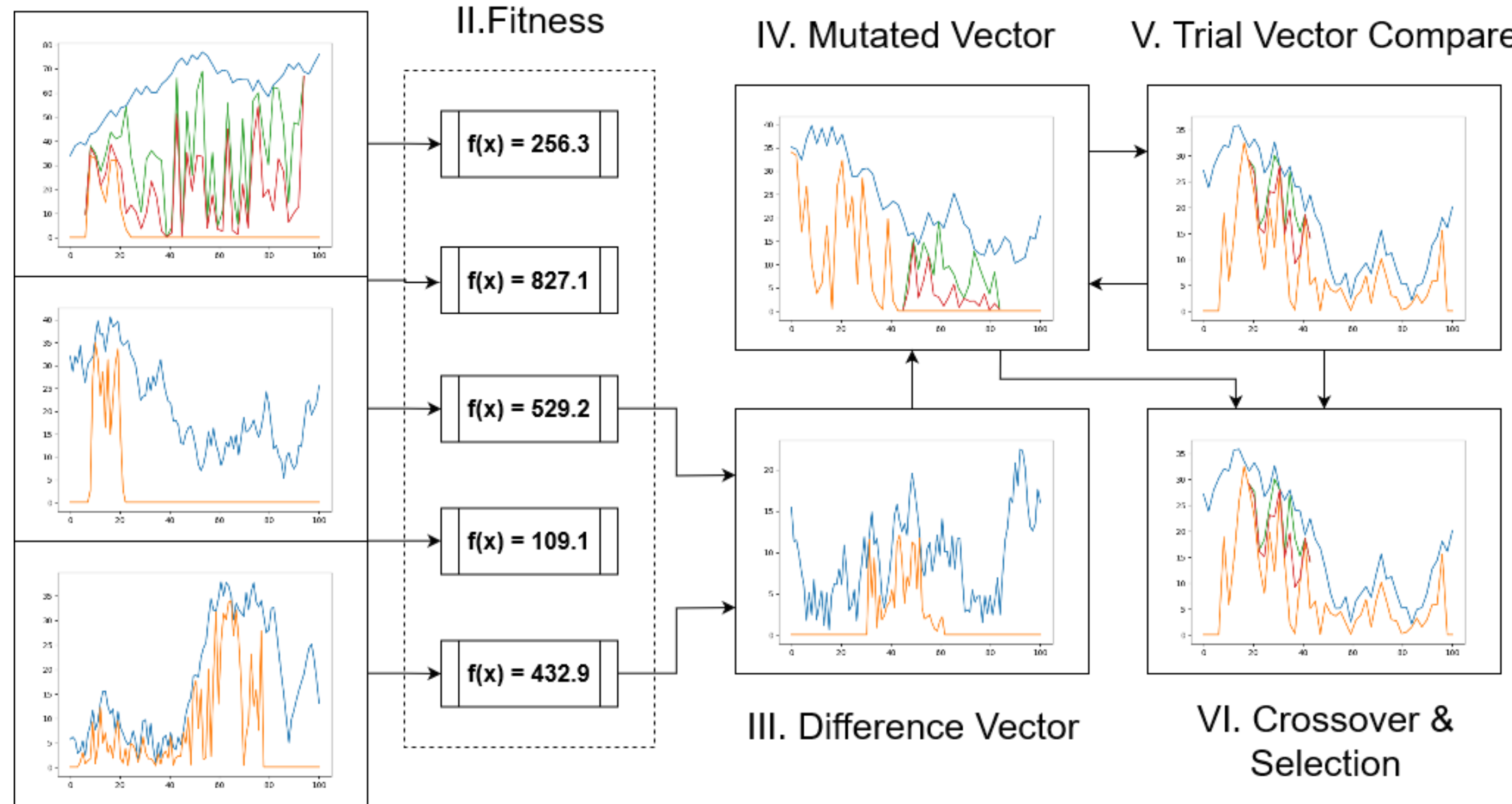


Figure 6: Flow diagram of one generation of the basic differential evolution algorithm. This is repeated for a specified number of generations, or until a desired fitness value is reached.

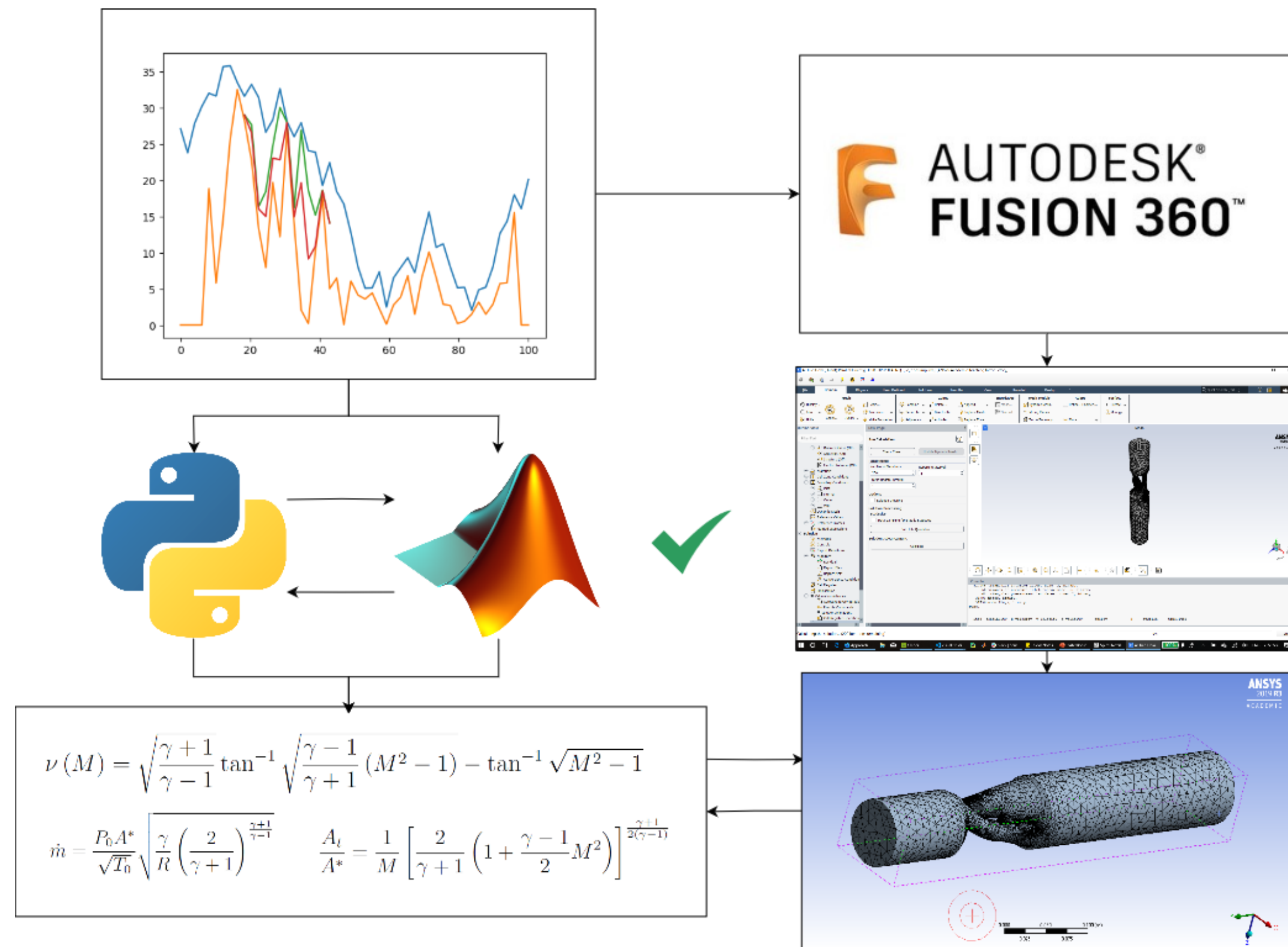


Figure 8: The multi-objective fitness function. The pseudo-function (left) is compared with the ground-truth-function (right) for verification.

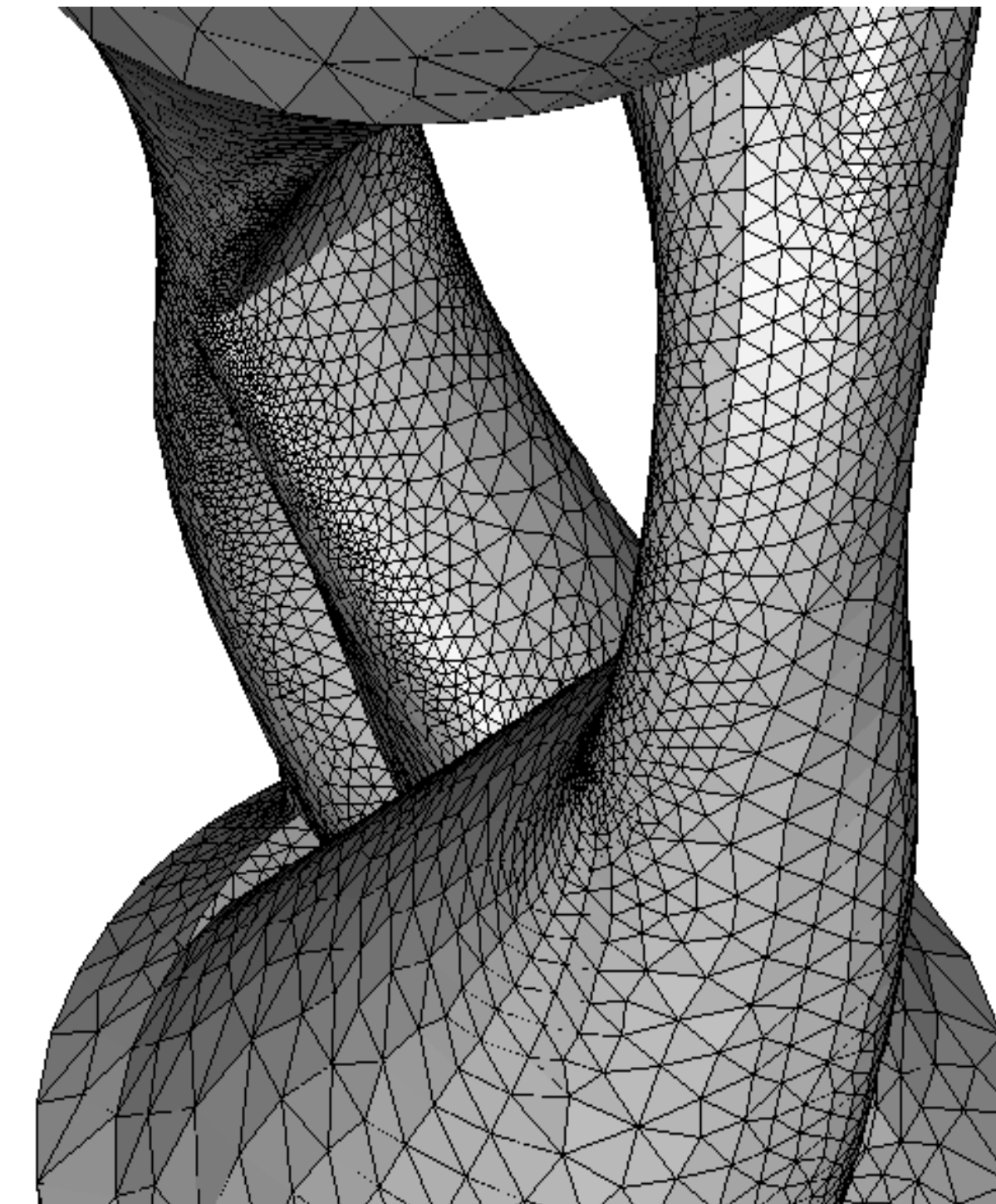


Figure 7: A tetrahedron mesh used for a computational fluid dynamics (CFD) simulation.

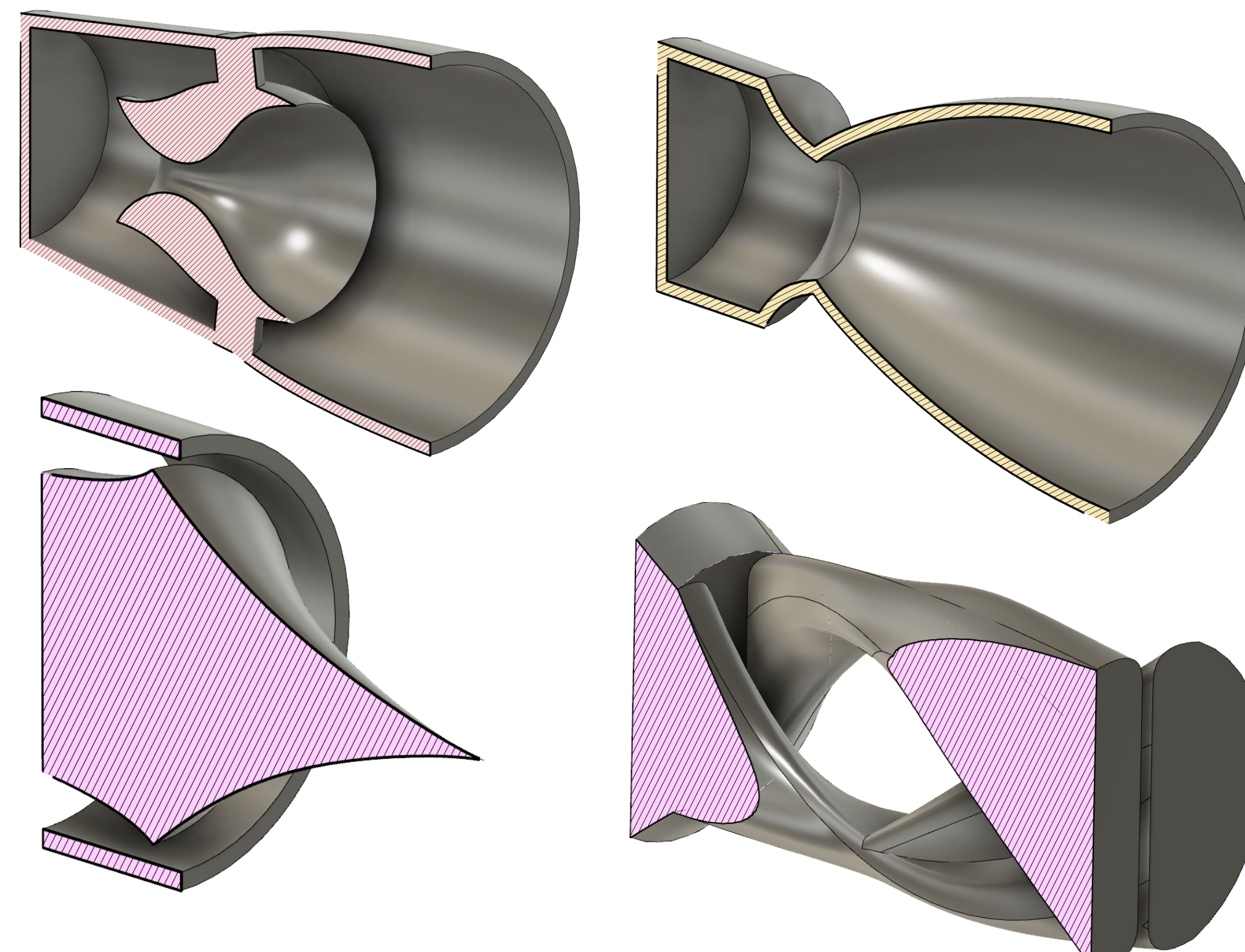
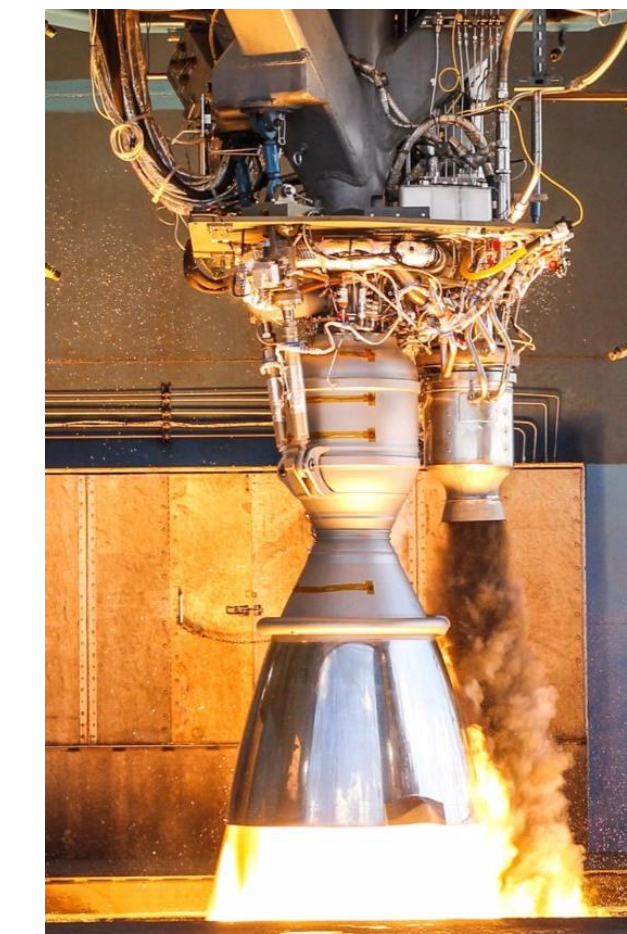


Figure 9: Four resultant nozzles generated from the DE algorithm. Left to right: Leaf nozzle, MOC nozzle, toroidal aerospike nozzle, spiral helix nozzle.

Sutton, G. P., & Biblarz, O. (2017). Rocket propulsion elements (9th ed.). Hoboken, NJ: John Wiley & Sons.
Yan, S., Li, B., Li, F., & Li, B. (2017). Finite element model updating of liquid rocket engine nozzle based on modal test results obtained from 3-D SLDV technique. Aerospace Science and Technology, 69, 412-418.
Balabel, A., Hegab, A.M., Nasr, M., & El-Beheery, S.M. (2011). Assessment of turbulence modeling for gas flow in two-dimensional convergent-divergent rocket nozzle. Applied Mathematical Modelling, 35, 3408-3422.
Yunusak, M., & Eyi, S. (2012). Design optimization of rocket nozzles in chemically reacting flows. Computers & Fluids, 65, 25-34. <https://doi.org/10.1016/j.compfluid.2012.05.002>
Storn, R., & Price, K. (1997). Differential evolution – A simple and efficient heuristic for global optimization over continuous spaces. Journal of Global Optimization, 11, 341-359. <https://doi.org/10.1023/A:1008202821328>.
Olson, C. C. (2019). Automated design of optical architectures using novel encoding methods and a multi-objective optimization framework. SPIE Proceedings, 11105. Retrieved from International Society for Optics and Photonics database.

Included the following four values: sum of the magnitudes of oblique and normal shocks, the sum of squared pressure gradients (more abrupt changes in pressure are discouraged), the standard deviation of said gradients, and the final exit velocity of the exhaust gases. Expansion fan propagation is also considered, i.e. the Method of Characteristics (MOC), which is the technique used by most engines today (Figure 5).

Once a specified number of generations is reached, CFD is used as the fitness function for a more accurate heuristic. The overall fitness function framework is summarized in Figure 8. For CFD simulations, parameters from SpaceX's Merlin 1D engine were used as follows:



MERLIN 1D (VAC) ENGINE	
Propellants	LOX/RP1
Chamber Pressure	9.7 MPa
Oxidizer/Fuel Ratio	2.56
Combustion Temperature	3670 K
Molecular Weight	23.3 kg/m
Ratio of Specific Heats	1.24

Figure 10: SpaceX's Merlin 1D parameters, as was used in CFD simulations.

IV. RESULTS

Figure 7 shows the four resultant nozzle geometries with maximum fitness scores in most objective categories. Table 1 shows the scores and parameters for these geometries.

Name	V_{exit} (m/s)	TKE (m/s ²)	SSPG (Pa)	Shocks	I_{sp} (VAC) (s)
LEAF	2615.6	5.282E3	3.2E6	220.9	329.1
MOC	2548.5	5.112E2	2.21E6	275.2	311.3
AERO	2612.3	7.719E2	2.78E6	254.9	325.1
HELIX	2517.0	2.419E5	9.12E5	109.3	326.8

Table 1: Objective values for four nozzle types. Shocks was a custom parameter.

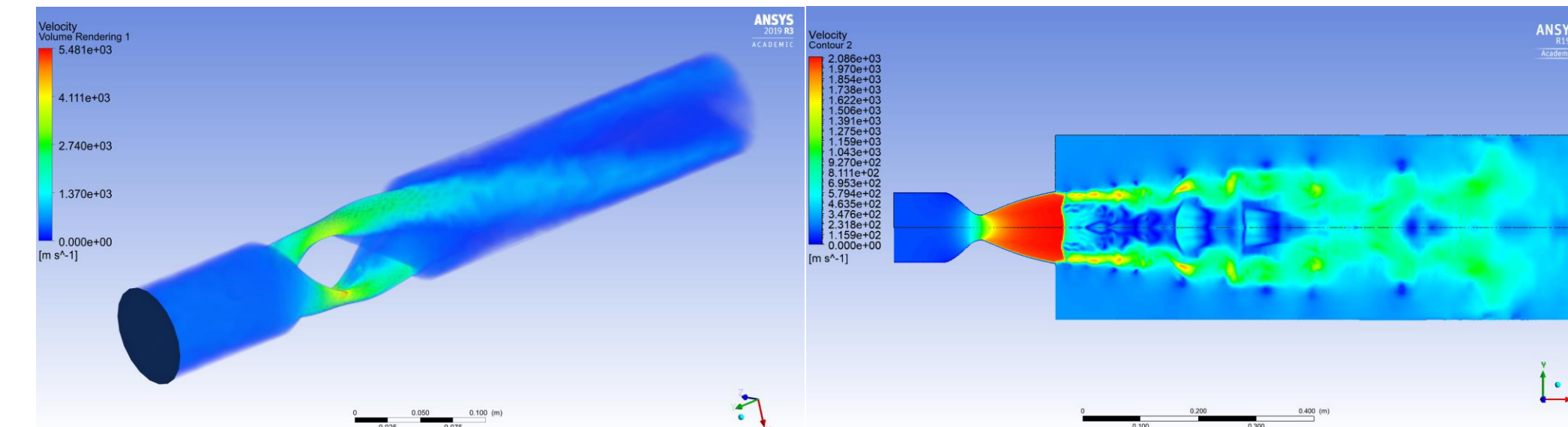


Figure 11: CFD postprocessing renderings of a helix and MOC nozzle.

As seen from Table 1, the leaf and helix nozzles seem to outperform the traditional MOC and aerospike nozzles in some areas. Though the helix and leaf nozzles seem to suffer from greater pressure gradients and larger magnitudes of turbulence kinetic energy, their final I_{sp} yields greater. It is suspected that this is due to superior shock dissipation, and the angular component introduced into the helix nozzle may choke the flow more steadily and allow for better combustion characteristics. Another consideration includes the engineering practicality of nozzles. The aerospike is not used widely today due to excessive heating on the inner spike and is something the leaf nozzle may also suffer from. The helix nozzle, however, may remedy this with large surface internal areas available for regenerative cooling.

V. CONCLUSION

The nearly 5% increase in specific impulse observed by initial CFD analysis is significant. Using parameters from SpaceX's Falcon 9 (FT) launch vehicle and the Tsiolovsky rocket equation

$$M_{fn} - M_f = M_{0n} e^{\frac{\Delta v}{I_{sp}^* g}} - M_0 e^{\frac{\Delta v}{I_{sp}^* g}} \approx 5.64E5 \text{ kg}$$

there is a per-launch weight saving of around 564 metric tonnes, which can amount to a conservative estimate of more than a million dollars saved per launch. For further experimentation, more general methods of generating a diverse initial population should be implemented since it is suspected the search space is far deeper than what was explored. In addition, more methods should be performed to validate these results.